Mitochondrial metabolism during daily torpor in the dwarf Siberian hamster: role of active regulated changes and passive thermal effects

Jason C. L. Brown, Alexander R. Gerson and James F. Staples

Am J Physiol Regul Integr Comp Physiol 293:R1833-R1845, 2007. First published 5 September 2007; doi:10.1152/ajpregu.00310.2007

American Journal of Physiology - Regulatory, Integrative and Comparative Physiology publishes original investigations that illuminate normal or abnormal regulation and integration of physiological mechanisms at all levels of biological organization, ranging from molecules to humans, including clinical investigations. It is published 12 times a year (monthly) by the American Physiological Society, 9650 Rockville Pike, Bethesda MD 20814-3991. ISSN: 0363-6119, ESSN: 1522-1490. Visit our website at http://www.the-aps.org/.

Am J Physiol Regul Integr Comp Physiol 293: R1833–R1845, 2007.
First published September 5, 2007; doi:10.1152/ajpregu.00310.2007.

Mitochondrial metabolism during daily torpor in the dwarf Siberian hamster: role of active regulated changes and passive thermal effects

Jason C. L. Brown, Alexander R. Gerson, and James F. Staples

Department of Biology, University of Western Ontario, London, Ontario, Canada

Submitted 1 May 2007; accepted in final form 27 August 2007

Brown JCL, Gerson AR, Staples JF. Mitochondrial metabolism during daily torpor in the dwarf Siberian hamster: role of active regulated changes and passive thermal effects. *Am J Physiol Regul Integr Comp Physiol* 293: R1833–R1845, 2007. First published September 5, 2007; doi:10.1152/ajpregu.00310.2007.—During daily torpor in the dwarf Siberian hamster, *Phodopus sungorus*, metabolic rate is reduced by 65% compared with the basal rate, but the mechanisms involved are contentious. We examined liver mitochondrial respiration to determine the possible role of active regulated changes and passive thermal effects in the reduction of metabolic rate. When assayed at 37°C, *state 3* (phosphorylating) respiration, but not *state 4* (nonphosphorylating) respiration, was significantly lower during torpor compared with normothermia, suggesting that active regulated changes occur during daily torpor. Using top-down elasticity analysis, we determined that these active changes in torpor included a reduced substrate oxidation capacity and an increased proton conductance of the inner mitochondrial membrane. At 15°C, mitochondrial respiration was at least 75% lower than at 37°C, but there was no difference between normothermia and torpor. This implies that the active regulated changes are likely more important for reducing respiration at high temperatures (i.e., during entrance) and/or have effects other than reducing respiration at low temperatures. The decrease in respiration from 37°C to 15°C resulted predominantly from a considerable reduction of substrate oxidation capacity in both torpid and normothermic animals. Temperature-dependent changes in proton leak and phosphorylation kinetics depended on metabolic state; proton leakiness increased in torpid animals but decreased in normothermic animals, whereas phosphorylation activity decreased in torpid animals but increased in normothermic animals. Overall, we have shown that both active and passive changes to oxidative phosphorylation occur during daily torpor in this species, contributing to reduced metabolic rate.

oxidative phosphorylation; proton conductance; *Phodopus sungorus*; top-down elasticity analysis

DESPITE THE POTENTIAL ADVANTAGES offered by homeothermy (43), the high metabolic rate (MR) associated with it can be costly. Periods of reduced food availability may make it difficult to support a high MR, and, furthermore, animals with a higher MR often have a shorter lifespan, possibly from increased rates of free radical production (70). Therefore, it may be beneficial for some mammals to periodically reduce their MR to avoid these potential problems. Hibernation and daily torpor are two strategies used by some mammals to reduce MR and its associated costs; for example, longevity in Turkish hamsters (45) and bats (71) has been shown to correlate with duration of hibernation. The reduction in MR during hibernation can last for several days or weeks, whereas the reduction in MR during daily torpor lasts for <24 h (46). Hibernators and daily heterotherms reduce MR to about 5% and 30% of basal MR, respectively (24), but since most mammals enter torpor at ambient temperatures below the thermoneutral zone, the reduction of MR during torpor is even greater compared with resting normothermic levels in cold environments. Furthermore, the reduction of MR occurs concomitantly with a reduction of body temperature (T_b).

There are four mechanisms that may contribute to the MR reduction during torpor (29): *1*) changes in whole animal thermal conductance; *2*) cessation of thermogenesis due to the resetting of the thermoregulatory set point; *3*) passive thermal effects as T_b falls; and *4*) active regulated changes to metabolic pathways. The extent of involvement of each of these mechanisms has been the focus of much controversy for many decades.

Whether thermal conductance is reduced and contributes to the reduced MR during torpor is not clear (24, 53, 63). Some authors have even proposed that thermal conductance may be increased during entrance into torpor to facilitate passive thermal effects on MR, but torpid animals are often curled up in nests (35) or in groups, as in marmots (2) and skunks (40), which should minimize thermal conductance. With regard to the cessation of thermogenesis, it seems well accepted that the thermoregulatory set point is gradually lowered at entrance into torpor (21), and this results in a decline of MR from resting to basal levels as facultative thermogenesis ceases. Most of the debate, however, has centered on the relative contributions of active regulated changes and passive thermal effects as mechanisms to reduce MR below basal levels.

It has been suggested that passive thermal effects are more important than any active regulated changes during hibernation and daily torpor, based on relatively low the fractional change in MR with a 10°C change in T_b (Q_{10}) values of 2.87 and 2.5, respectively, comparing MR and T_b values (29) from normothermia and steady-state torpor. By contrast, it has also been suggested that passive thermal effects have no role in hibernation or daily torpor and that active downregulation of metabolism is the sole mechanism of MR reduction because it allows for greater degrees of metabolic suppression and reduces heat energy waste (35). More recently, one study suggested that daily heterotherms rely mostly upon passive thermal effects (average Q_{10} of 2.3) and hibernators rely upon a combination of passive thermal effects and active regulated changes (Q_{10} between 3 and 6), although body size and ambient temperature could affect this generalization (24). Yet another study proposed a synergistic role for both passive thermal effects and

Address for reprint requests and other correspondence: J. F. Staples, Dept. of Biology, Univ. of Western Ontario, London, ON, N6A 5B7, CANADA (e-mail: jfstaple@uwo.ca).

The costs of publication of this article were defrayed in part by the payment of page charges. The article must therefore be hereby marked "*advertisement*" in accordance with 18 U.S.C. Section 1734 solely to indicate this fact.

active regulated changes in both daily torpor and hibernation, although the extent of contribution of each mechanism differs between hibernation and daily torpor (37). Therefore, the entire gamut of relative contributions, from entirely passive to entirely active, has been proposed in the literature for both hibernation and daily torpor.

The studies cited in the preceding paragraph were based on whole animal measurements of MR and T_b. Studies of the respiration rates of isolated mitochondria, which are responsible for about 90% of whole animal oxygen consumption (61), have demonstrated active, regulated inhibition during hibernation in liver mitochondria (3, 11, 20, 23, 50, 52, 55) but not skeletal muscle mitochondria (3, 52). This tissue-specific occurrence of active regulated changes might explain the conflict between whole animal and mitochondrial studies (3). To our knowledge, comparable studies on mitochondria from daily heterotherms are entirely lacking, and, in addition, only some of these mitochondrial studies of hibernators have simultaneously considered the role of passive thermal effects (52, 55) with disparate results.

The purpose of the present study, therefore, was to investigate changes in liver mitochondrial respiration during daily torpor in the dwarf Siberian hamster, *Phodopus sungorus*. Liver respiration is a significant contributor to basal MR (12–17%; 49) despite the fact that it represents only 5% of body weight in mammals of this size (20–40 g) (64). In particular, we were interested in two objectives: *1*) to determine whether liver mitochondrial respiration was reduced during daily torpor by active regulated changes and/or passive thermal effects, and *2*) if a role for either mechanism could be demonstrated, to determine the components of oxidative phosphorylation (OxPhos) which were affected and the extent to which they contributed to changes in mitochondrial respiration. In this way, this study represents the first comprehensive examination of the role of both active and passive changes on mitochondrial respiration during daily torpor and the site of action of each mechanism.

Our objectives were met simultaneously through the use of top-down elasticity analysis (hereafter, elasticity analysis). Elasticity analysis has been used quite extensively in the past decade to study the impact of various effectors on OxPhos, including thyroid hormones (33, 44), pharmacologically-important compounds (12), temperature (14, 18), and hibernation (3), as well as other natural forms of hypometabolism (4, 65). Simply, elasticity analysis views OxPhos as a system consisting of three components: substrate oxidation, ADP phosphorylation, and proton leak. These are interrelated by the proton motive force (ΔP): the substrate oxidation component generates ΔP, and the phosphorylation and proton leak components consume it. To determine whether a given effector influences a component of OxPhos, one must determine whether the effector evokes a kinetic change in that component (8). In our study, we were examining two effectors: metabolic state (normothermic vs. torpid) and temperature [37°C vs. 15°C; the former temperature is physiological for normothermic animals, and the latter temperature represents the lowest T_b during torpor in this species (41)].

Using this approach, we have demonstrated that liver mitochondrial respiration is reduced during daily torpor by active regulated changes but only when measured at high temperature. At low temperatures, passive thermal effects become more important. The active changes involved the substrate oxidation and proton leak components of OxPhos, whereas the passive changes involved all three components.

MATERIALS AND METHODS

Animals. This project was approved by the local Animal Use Subcommittee (protocol no. 2004-055-06). Dwarf Siberian hamsters were obtained from a breeding colony maintained by Dr. Katherine Wynn-Edwards at Queens University, Kingston, ON, Canada. They were housed singly in plastic cages (12 × 18 × 28 cm) with Beta Chips for bedding and two 2-inch squares of compressed nesting material (Ancare), which they readily converted to nests. They were fed a high-polyunsaturated diet (5.5 mg linoleic acid/g diet; TestDiets, Richmond IN) and water ad libitum. This diet was selected because dwarf Siberian hamsters have been shown to prefer an unsaturated diet at low ambient temperatures (38), and no torpor was observed in one cohort of animals that were fed a standard rodent diet (Brown JCL, unpublished observation). They were maintained at 18°C with a photoperiod of 14:10-h light-dark cycle for 4 wk. Subsequently, the temperature and photoperiod were changed to 15°C and 8:16-h light-dark cycle, respectively, and maintained for 3 to 5 mo to induce daily torpor.

T_b measurement. To measure T_b, radiotelemeters (model TA-F20; Data Sciences International, Arden Hills, MN) were implanted intraperitoneally under isofluorane anesthesia. Postoperative analgesia (subcutaneous buprenorphrine, 0.03 mg/ml, 0.1 ml/100 g) was administered twice daily for 3 days. T_b was recorded every 5 min using telemetry receivers (models RA1010 and RPC-1; Data Sciences International) with data acquisition software and hardware (Dataquest ART; Data Sciences International).

Animal sampling and mitochondrial isolation. Animals were considered torpid if T_b was below 31°C for at least 30 min (15), and torpid animals were sampled 2 to 3 h into a torpor bout. All animals were similarly aged (between 4 and 8 mo) at the time of sampling. Normothermic animals were killed by anesthetic overdose (Euthanyl, 270 mg/ml, 0.2 ml/100 g ip), whereas torpid animals were killed by cervical dislocation to minimize arousal. Euthanyl has been shown to have no effect on mitochondrial metabolism (67). The liver was removed quickly. A small portion (75–150 mg) of liver was immediately frozen in liquid nitrogen and stored at −80°C, and the remainder was used immediately for mitochondrial isolation. Mitochondria were isolated using a previously published protocol (52). The liver was rinsed with ice-cold homogenization buffer (HB; 250 mM sucrose, 10 mM HEPES, 1 mM EGTA, 1% fatty-acid-free BSA, pH 7.4 at 4°C) and then cut into small pieces on ice in HB and homogenized using three passes of a loose-fitting Teflon pestle at 100 rpm in a 30-ml glass mortar. The homogenate was filtered through one layer of cheesecloth and centrifuged at 1,000 *g* for 10 min at 4°C in polycarbonate centrifuge tubes. Floating lipid was aspirated from the supernatant, which was then filtered through four layers of cheesecloth and centrifuged again at 1,000 *g* for 10 min at 4°C. Once again, floating lipid was aspirated from the supernatant and filtered through four layers of cheesecloth; then, the supernatant was centrifuged at 8,700 *g* for 10 min at 4°C. The supernatant and adhering lipid were removed, and the light pellet fraction was also removed as much as possible. The dark pellet was resuspended in 30 ml HB and centrifuged at 8,700 *g* for 10 min at 4°C. The supernatant and adhering lipid were removed again, and the final pellet was resuspended in 500 μl of ice-cold HB and kept on ice until assayed.

Mitochondrial respiration rate and membrane potential. Mitochondrial respiration rates were measured using temperature-controlled polarographic O_2 meters (Dual Digital model 20; Rank Brothers, Bottisham, UK) in 2 ml [for flux and adenine nucleotide translocator (ANT) determinations] or 3 ml (for elasticity analysis) of assay buffer (225 mM sucrose, 20 mM HEPES, 10 mM KH_2PO_4, 1% BSA, pH 7.4 at 37°C). Oxygen electrodes were calibrated to ambient air,

using O_2 contents previously reported (58) and corrected for assay temperature and local atmospheric pressure. Unless otherwise stated, all compounds were dissolved in assay buffer.

For determinations of flux through various segments of the electron transport chain (ETC), mitochondria were added to a final concentration of ~0.2 mg protein/ml. Flux was determined under *state 3* conditions (0.5 mM ADP) at 37°C; this concentration of ADP was sufficient to support *state 3* respiration for the period of time required to complete the required measurements. For flux through complexes I–IV, glutamate (5 mM) and malate (1 mM) were added. After steady-state rates were acquired, rotenone (2 μg/ml, dissolved in ethanol) was added to inhibit complex I. Subsequently, succinate (6 mM) was added to stimulate flux through complexes II–IV. Malonate (5 mM) was added to competitively inhibit succinate oxidation, and decylubiquinol (0.75 mM, dissolved in ethanol), prepared according to Trounce et al. (69), was added to stimulate flux through complexes III and IV. In excess, the oxidation of decylubiquinol does not involve endogenous ubiquinone (42). Complex III was then inhibited by the addition of antimycin A (10 μg/ml, dissolved in ethanol), and, subsequently, ascorbate (8 mM) and *N*,*N*,*N*′,*N*′-tetramethyl-*p*-phenylenediamine (TMPD; 0.8 mM) were added to measure flux through complex IV.

For the determination of the kinetics of proton leak, simultaneous measurements of oxygen consumption and proton motive force (ΔP) are required. Rotenone (2 μg/ml, dissolved in ethanol) was added to inhibit complex I, and oligomycin (10 μg/ml, dissolved in ethanol) was added to inhibit ATP synthase (i.e., to inhibit the phosphorylation component of OxPhos). We measured mitochondrial membrane potential ($\Delta\Psi_m$) as an approximation of ΔP. In some other studies (3), nigericin has also been added to collapse ΔpH so that ΔP is fully expressed as $\Delta\Psi_m$; however, in the present study, nigericin was not used. This is appropriate as long as changes in ΔpH are negligible, which has been demonstrated for rat liver mitochondria (18, 51). To measure $\Delta\Psi_m$, we used tetraphenylphosphonium (TPP^+), a lipophilic cation, whose uptake by mitochondria is $\Delta\Psi_m$-dependent. A TPP^+-selective electrode (World Precision Instruments, Sarasota FL) was inserted into the O_2 electrode chamber to measure external TPP^+ concentration ($[TPP^+]$). The TPP^+ electrode was calibrated by making five additions of TPP^+; each addition increased external $[TPP^+]$ by 1 μM. Once calibrated, mitochondria were added to the chamber to a final concentration of 1.0 mg protein/ml at 37°C and 1.3 mg protein/ml at 15°C. Subsequently, succinate (6 mM) was added to stimulate *state 2* (approximating *state 4*) respiration. The kinetics of proton leak were determined by inhibiting the substrate oxidation component stepwise by adding malonate (5 additions, each of which increased the concentration of malonate by 0.5 mM in the assay buffer) and measuring the effect on $\Delta\Psi_m$. After the final malonate addition, CCCP (0.1 μM, dissolved in ethanol) was added to completely uncouple the mitochondria and allow for correction of electrode drift.

$\Delta\Psi_m$ was calculated from the external $[TPP^+]$ using a modified Nernst equation (*Eq. 1*), as in Barger et al. (3)

$$\Delta\psi_m = a \log\left(\frac{([TPP^+]_{added} - [TPP^+]_{external})(b)}{(v)(\text{mg protein})([TPP^+]_{external})}\right) \quad (1)$$

In *Eq. 1*, *a* is a temperature-dependent coefficient ($a = 2.3\ RT/F$, where R is the universal gas constant, T is absolute temperature, and *F* is the Faraday constant), *b* is a binding constant used to correct for nonspecific binding of TPP^+, and v is the mitochondrial matrix volume. The value of *b* was 0.16 (48) and the value of v was 0.001 ml/mg protein (31), both of which were determined for rat liver mitochondria. Although we did not determine whether mitochondrial volume changes with metabolic state and/or temperature, the effect of changes in mitochondrial volume is negligible when TPP^+ is used (62). We have also assumed that nonspecific binding of TPP^+ does not change with temperature. Although binding of TPP^+ to liposomal membranes composed of dipalmitoylphosphatidylcholine has been shown to be temperature dependent (16), it is not clear how temperature affects TPP^+ binding in mitochondria. Any such changes would not affect any differences we find between metabolic states when measured at the same temperature.

For determination of the kinetics of ADP phosphorylation, oxygen consumption and $\Delta\Psi_m$ were again measured simultaneously. Rotenone (2 μg/ml, dissolved in ethanol) was added to inhibit complex I. $\Delta\Psi_m$ was measured as described for proton leak kinetics. Once the TPP^+ electrode was calibrated, mitochondria were added to a final concentration of 0.7 mg/protein ml for 37°C and 1.0 mg/protein ml for 15°C. Succinate (6 mM) and ADP (1 mM) were added to stimulate *state 3* respiration; this concentration of ADP was sufficient to support *state 3* respiration for the period of time required to complete the required measurements. The kinetics of phosphorylation were determined by inhibiting the substrate oxidation component stepwise by adding malonate (5 additions to 0.33 mM each in assay). After the final malonate addition, as for proton leak kinetics, CCCP (0.1 μM) was added. The kinetics of the substrate oxidation component were not measured directly. Instead, they were represented by the straight line which connects the uninhibited *state 3* (from the phosphorylation kinetics) and uninhibited *state 4* (from the proton leak kinetics) measurements, as in Barger et al. (3).

ANT concentration. ANT concentration was determined polarographically (27). Rotenone (2 μg/ml, dissolved in ethanol) and succinate (5 mM) were added to a suspension of mitochondria (at a concentration of about 0.1 mg protein/ml). ADP (0.5 mM) was subsequently added to stimulate *state 3* respiration. *State 3* respiration was titrated with carboxyatractyloside (CAT), a noncompetitive inhibitor of ANT, by additions of 5 μl of 0.01 mM CAT. *State 3* respiration was gradually inhibited to the point that additions of CAT no longer decreased respiration rate. The resultant titration curve was plotted, and the concentration of ANT was determined from the point at which the line of steepest slope intersected the nearly horizontal line representing the fully inhibited state (for an example, see Fig. 7*A*). The concentration of CAT at this point was equal to the concentration of ANT in the mitochondrial suspension (27).

Enzyme assays. Immediately after the liver was removed from the animal, a small piece was flash frozen in liquid nitrogen and stored at −80°C to determine liver citrate synthase activity, a marker of mitochondrial density. In preparation for this assay, the frozen liver was thawed in 9 volumes of ice-cold grinding buffer (25 mM HEPES, 0.1% vol/vol Triton-X, 2 mM EDTA, pH 7.0 at 25°C), minced thoroughly with scissors, and homogenized (3 × 10 s) by using a tissue homogenizer (Tissue Tearor; Biospec). This homogenate was centrifuged at 4°C for 5 min at 2,000 *g*. For the assay, the reaction mixture contained 50 mM Tris (pH 8.0 at 37°C), 0.15 mM DTNB, and 0.15 mM acetyl coenzyme A. This reaction mixture was incubated for 5 min at 37°C for temperature equilibration. After the incubation, liver homogenate (30–40 μg protein) and oxaloacetate (to a final concentration of 0.33 mM) were added, and the reaction was followed at 412 nm for 5 min (ε = 13.6 mM/cm). Blanks (measured in the absence of oxaloacetate) were processed simultaneously, and the activity was expressed as mU/mg tissue protein and mU/g wet liver.

Complex I (NADH dehydrogenase) and complex II-III (succinate cytochrome *c* oxidoreductase) activity were determined on isolated mitochondria (66) that had been previously stored at −80°C. For complex I activity, the reaction mixture contained 25 mM KH_2PO_4 (pH 7.2 at 37°C), 0.2 mM NADH, 10 mM $MgCl_2$, and 1 mM KCN. Mitochondria (5–10 μg protein) were added, and the mixture was incubated at 37°C for 3 min for temperature equilibration. The reaction was initiated by the addition of decylubiquinone to a final concentration of 50 μM and read at 340 nm for 7 min (ε = 6.22 cm/mM). This measurement yields the rate of total NADH oxidation. The rate of rotenone-insensitive NADH oxidation was determined in the presence of 0.1 mM of rotenone. The difference between these rates yields the rate of rotenone-sensitive NADH oxidation, which

was interpreted as complex I activity. Blanks (buffer instead of homogenate) were processed simultaneously, and the activity was expressed as milliunits per milligram mitochondrial protein.

For complex II-III activity, the reaction mixture contained 100 mM KH_2PO_4 (pH 7.4 at 37°C), 0.3 mM EDTA, 1 mM KCN, and 100 μM cytochrome *c*. Mitochondria (5–10 μg) were added to this mixture, and it was incubated at 37°C for 3 min for temperature equilibration. The reaction was initiated by the addition of succinate to a final concentration of 70 mM and read at 550 nm for 7 min ($\varepsilon = 27.7$ mM/cm). This measurement yields the total rate of succinate/cytochrome *c* oxidoreductase activity. Malonate (to a final concentration of 140 mM) was added to competitively inhibit succinate oxidation in some reactions to determine the rate of reduction of cytochrome *c*, which is independent of succinate oxidation. The difference between these rates yields the activity of complex II-III. Blanks (buffer instead of homogenate) were processed simultaneously, and the activity was expressed as milliunits per milligram mitochondrial protein.

Protein determination. Protein concentration of liver homogenate and mitochondrial preparations was determined using the Bradford assay (Bio-Rad), according to the standard procedure for microtiter plates, with BSA as the standard.

Data analysis. Student's *t*-test was used to compare normothermic and torpid animals in terms of body mass and T_b at time of sampling, flux through each segment of the ETC, enzyme activity, and ANT concentration. For both *states 3* and *4* respiration data, separately, a one-way ANOVA and a Student-Newman-Keuls multiple comparison test were used to compare differences between normothermic and torpid animals at both assay temperatures and between assay temperatures.

Kinetic curves for substrate oxidation were fitted to a linear equation, whereas kinetic curves for both proton leak and phosphorylation were fitted to an exponential equation (single exponential, 3 parameters) using statistical software (SigmaPlot 2001). For the measurement of proton leak kinetics, since the phosphorylation component is inhibited (by oligomycin and lack of ADP), it can make no contribution to the measurements of proton leak kinetics; however, for the measurements of phosphorylation kinetics, the proton leak component cannot be similarly inhibited, and so this component does make some contribution to the experimental measurements of phosphorylation kinetics. To correct for this contribution of the proton leak component on phosphorylation kinetics, for each value of $\Delta\Psi_m$ measured for the phosphorylation component, the oxygen consumption rate due to proton leak was calculated using the equation fitted to the proton leak kinetics and subtracted from the oxygen consumption rate measured for phosphorylation kinetics. This approach, used in previous studies (14), showed that proton leak usually accounted for <10% of *state 3* respiration regardless of temperature, except for mitochondria isolated from torpid animals measured at 15°C, where proton leak accounted for 25% of *state 3*.

Measurements of the kinetics of all components of OxPhos allowed us to quantitatively assess changes in kinetics. Flux control and elasticity coefficients for *states 3* and *4* mitochondrial respiration were calculated according to Hafner et al. (30), using the mean kinetic data, and, based on these coefficients and the observed changes in ΔP and flux through the components between metabolic states and/or temperature, we calculated integrated elasticity coefficients and integrated partial response coefficients, based on Ainscow and Brand (1). Integrated elasticity coefficients are a quantitative indicator of changes in kinetics between metabolic states and/or temperature since they are calculated by comparing the observed change in flux through a particular component to the predicted change in flux based on the elasticity of the component to ΔP and the observed change in ΔP. If the integrated elasticity coefficient for a component is different from zero, then we assume that a kinetic change in that component explains why the observed change in flux is different from what we would have predicted. The impact of a kinetic change in a component of OxPhos, however, is dependent upon the control of that component over respiration. Partial integrated response coefficients reflect this notion since they are calculated as the product of the integrated elasticity coefficient and the flux control coefficient for the component.

RESULTS

Animals were exposed to short photoperiod (8:16-h light-dark cycle) for about 3 mo before daily torpor was observed. The occurrence of daily torpor was determined by measuring T_b (Fig. 1), and torpor was said to occur when T_b was below 31°C for at least 30 min (15). Therefore, in our study, torpid animals were sampled 2 to 3 h into a torpor bout, about 1.5 to 2.5 h after the beginning of the photophase. Normothermic animals were sampled at the same time of day as torpid animals, but their T_b was significantly higher (Table 1). None of the normothermic animals had previously experienced a torpor bout, but all animals were observed to undergo a change in fur coloration, from grey to white, which has been reported to occur in response to short photoperiod acclimation in this species (34). At the time of sampling, torpid animals weighed significantly less than normothermic animals, but mitochondrial density, as determined by citrate synthase activity, was not different between the metabolic states (Table 1).

Our first objective was to determine whether there was a role for active regulated changes and/or passive thermal effects on liver mitochondrial respiration during daily torpor. When measured at 37°C, we found that *state 3* respiration was significantly reduced by 30% in mitochondria isolated during torpor compared with those isolated during normothermia, but *state 4* respiration was not different between normothermia and torpor

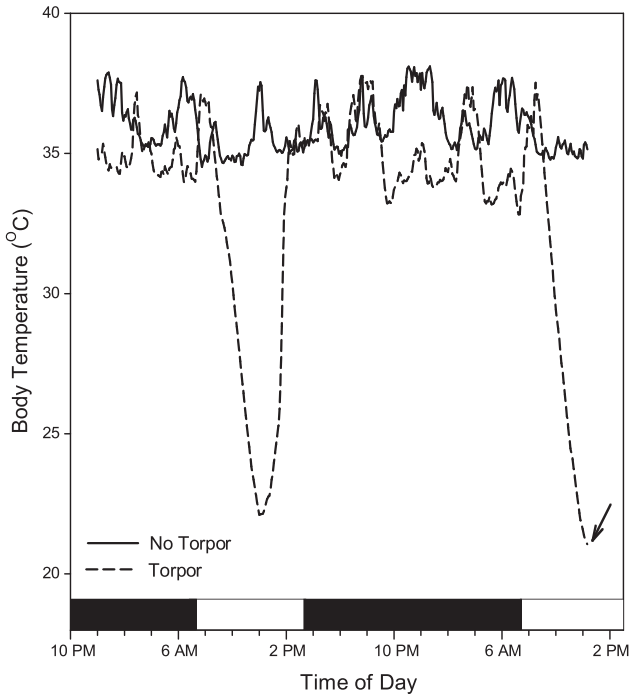

Fig. 1. Body temperature of 2 hamsters over the same 40-h period. One hamster remained normothermic over this time period, whereas the other hamster showed 2 bouts of daily torpor. The arrow indicates the time point at which the torpid hamster was sampled. The black horizontal bars indicate the scotophase (16 h, lights off at 15:30 EST), and the white horizontal bars indicate the photophase (8 h, lights on at 7:30 EST). Animals entered torpor at the beginning of the photophase and were fully aroused before the beginning of scotophase.

Table 1. *Body mass, body temperature, and citrate synthase activity of animals used in this study at time of sampling*

	Normothermic	Torpid	*P* Value
n	16	8	
Body mass, g	35.4±5.2	27.2±3.0	<0.001
Body Temperature, °C	35.7±1.9	22.8±1.2	<0.001
Citrate synthase			
mU/mg protein	64.7±5.0	67.5±21.0	0.777
mU/g wet liver	11.2±1.3	12.3±4.0	0.584

Values are means ± SD. Student's *t*-test was used to compare normothermic and torpid animals for each parameter.

(Fig. 2). These results suggested that some active regulated changes did occur during daily torpor. When measured at 15°C, mitochondrial respiration was significantly lower compared with 37°C for both normothermic and torpid animals; however, neither *state 3* nor *state 4* respiration was different between normothermia and torpor at this temperature (Fig. 2). This suggested that passive thermal effects also play a significant role in reducing mitochondrial respiration during daily torpor, and, in addition, that the active regulated changes are temperature-dependent (i.e., they are not observed at low temperatures).

After having demonstrated that both active regulated changes and passive thermal effects were involved in the reduction of liver mitochondrial respiration during daily torpor, we evaluated how each component of OxPhos contributed to the active and passive changes in mitochondrial respiration. To determine where the active regulated changes occurred, the kinetics of the components of OxPhos were determined and compared at 37°C for mitochondria isolated from both normothermic and torpid animals. For proton leak (Fig. 3*A*), the kinetic curve for torpid mitochondria was shifted to the left, such that, for any value of $\Delta\Psi_m$, the mitochondrial respiration rate was greater in torpid mitochondria compared with normothermic mitochondria. For substrate oxidation (Fig. 4*A*), the kinetic curve for torpid mitochondria was shifted downward, and, therefore, respiration of torpid mitochondria was lower at any given value of $\Delta\Psi_m$ compared with normothermic mitochondria. By contrast, for phosphorylation (Fig. 5*A*), for all values of $\Delta\Psi_m$, mitochondrial respiration rate was the same for

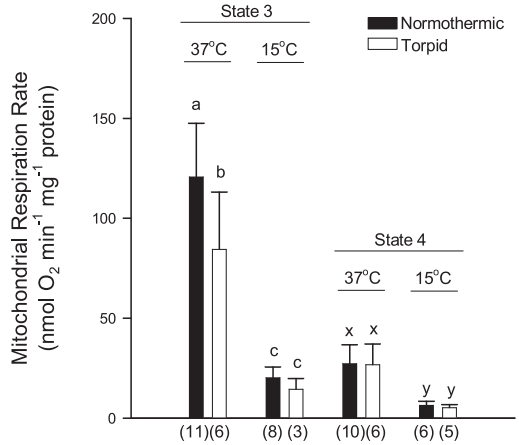

Fig. 2. Respiration of liver mitochondria isolated from normothermic and torpid animals measured at 37°C and 15°C with 6 mM succinate as substrate. For each respiration state (*states 3* and *4*), significantly different values are indicated by different letters. For *state 3*, for all pairwise comparisons, P is <0.01, except for the comparison between normothermia and torpor at 15°C for which $P = 0.70$. For *state 4*, for all pairwise comparisons, P is <0.001, except for the comparisons between normothermia and torpor, at both 37°C and 15°C, for which $P = 0.90$ and $P = 0.80$, respectively. Values are means ± SD. The number of samples for each value is indicated in parentheses below the corresponding bar.

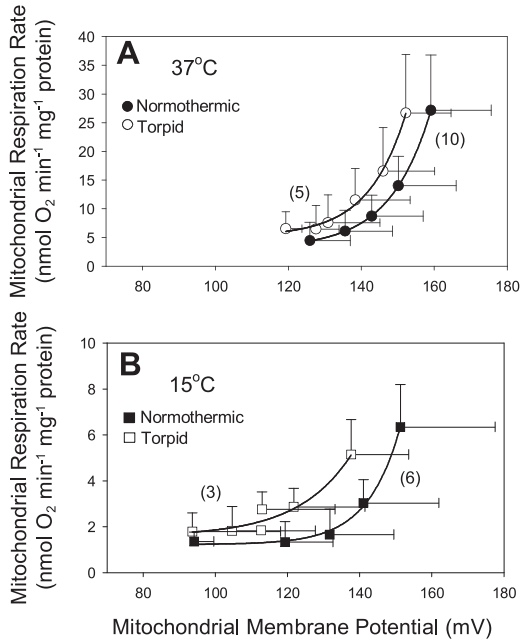

Fig. 3. Kinetics of mitochondrial proton leak at (*A*) 37°C and (*B*) 15°C for liver mitochondria from animals sampled in normothermia and torpor. The number of samples for each curve is shown in parentheses beside the curve. Values are means ± SD.

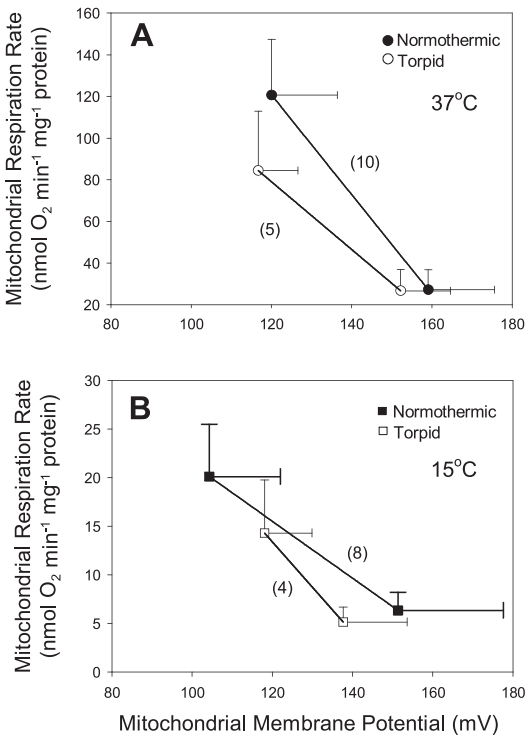

Fig. 4. Kinetics of substrate oxidation at 37°C (*A*) and 15°C (*B*) for liver mitochondria from normothermic and torpid animals. The number of samples for each curve is shown in parentheses beside the curve.

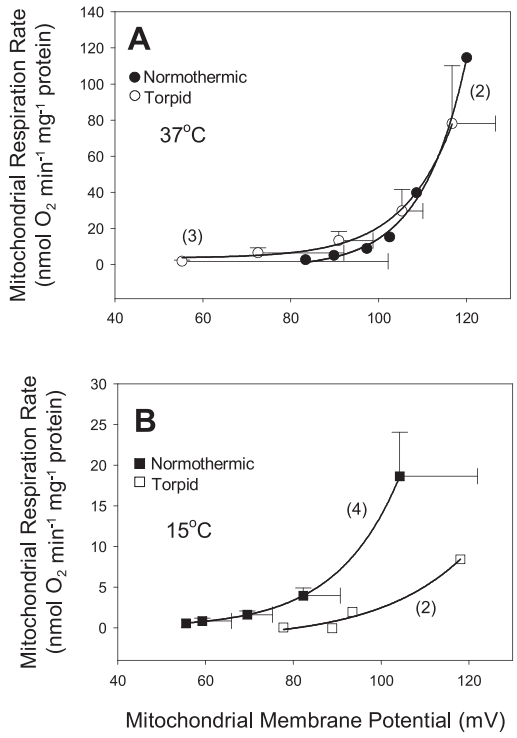

Fig. 5. Kinetics of phosphorylation at 37°C (*A*) and 15°C (*B*) for liver mitochondria from normothermic and torpid animals. The number of samples for each curve is shown in parentheses beside the curve. Values are means ± SD, except where there were only 2 samples, in which case SD could not be calculated.

both metabolic states; that is, the kinetic curves overlapped. From these kinetic measurements, we calculated elasticity and flux control coefficients for each component of OxPhos for both *state 3* and *state 4* respiration according to Hafner et al. (30) (Table 2). Using the elasticity coefficients, and the measurements of mitochondrial respiration and membrane potential, we then calculated integrated elasticity coefficients for the transition from normothermia to torpor according to Ainscow and Brand (1). These coefficients allowed us to quantitatively determine any differences in the kinetics of the components of OxPhos between the metabolic states. Then, using these integrated elasticity coefficients and the flux control coefficients, we calculated partial integrated coefficients, which show the contribution that a change in kinetics of a particular component has on mitochondrial respiration. The sum of the partial integrated coefficients for all components of OxPhos for a given state of respiration yields the integrated response coefficient, which describes the overall percent change in respiration rate. This analysis is summarized in Table 2.

Our analysis has shown that the active reduction of *state 3* respiration during daily torpor was achieved entirely by an inhibition of substrate oxidation capacity; that is to say, phosphorylation capacity was not reduced during torpor. Furthermore, the lack of reduction of *state 4* respiration during torpor occurred because the proton leakiness of the inner mitochondrial membrane (IMM) was significantly increased, which offset the decreased substrate oxidation capacity.

After having determined that substrate oxidation and proton leakiness underwent active regulated changes during torpor, we decided to further investigate the nature of these changes. For substrate oxidation, we measured *state 3* respiration at 37°C using various substrates that donate their electrons to the ETC at different points. The various substrates included glutamate/malate, succinate, decylubiquinol, and TMPD/ascorbate. The oxidation of glutamate produces NADH (via glutamate dehydrogenase), which is oxidized through complex I → ubiquinone → complex III → cytochrome *c* → complex IV. Some succinate is generated by glutamate oxidation, but its contribution to glutamate respiration is negligible, since the addition of rotenone essentially eliminates respiration on glutamate. Succinate is oxidized through complex II → ubiquinone → complex III → cytochrome *c* → complex IV. Decylubiquinol, an ubiquinol analog, donates electrons directly to complex III → cytochrome *c* → complex IV. TMPD is oxidized directly by cytochrome *c* → complex IV and, itself, is maintained in a reduced state by ascorbate. *State 3* respiration on glutamate and succinate was significantly reduced in mitochondria from torpid animals by ~70% and 33%, respectively; respiration rates on decylubiquinol and ascorbate/TMPD showed no significant reduction in torpid animals (Fig. 6). These data suggest that the site of inhibition of substrate oxidation is upstream of complex III.

To further examine the nature of the inhibition of substrate oxidation, we assayed the maximal activity of two enzyme complexes, complex I and complex II-III, using isolated mitochondria. Since this latter enzyme activity is dependent upon endogenous ubiquinone (42), these two enzyme activities represent the entire portion of the ETC where our respiration data suggested the inhibition occurs. However, neither complex I [normothermia, 22.6 mU/mg protein (SD 5.9, $n = 4$); torpor, 18.9 mU/mg protein (SD 8.8, $n = 4$, $P = 0.43$)], nor complex II-III (normothermia, 28.2 mU/mg protein (SD 3.6, $n = 4$); torpor, 35.8 mU/mg protein (SD 8.3, $n = 4$)] showed any significant difference in maximal activity between normothermia and torpor ($P = 0.502$ and $P = 0.147$ for complex I and II-III, respectively).

For proton leakiness, it was recently reported that the concentration of the ANT may be a contributor of proton leak (9), so we measured the concentration of ANT (Fig. 7*A*) to determine whether it could explain the active regulated increased leakiness of the IMM during daily torpor. However, we found that during daily torpor, the concentration of ANT was unchanged (Fig. 7*B*).

To determine where the passive thermal effects occurred, we determined the kinetics of the components of OxPhos at 15°C (proton leak, Fig. 3*B*; substrate oxidation, Fig. 4*B*; phosphorylation, Fig. 5*B*) and compared them to those at 37°C. For proton leak and substrate oxidation, the kinetic curves measured at 15°C were shifted downward compared with those measured at 37°C, such that, at any given value of $\Delta\Psi_m$, the mitochondrial respiration rate was lower at 15°C. For phosphorylation, the effect of temperature on the kinetic curves differed between the metabolic states. For normothermia, the phosphorylation kinetic curves measured at 37°C and 15°C overlapped, so there was no difference in mitochondrial respiration rate at any value of $\Delta\Psi_m$, whereas for torpor, the kinetic curve measured at 15°C was shifted downward such that at any value of $\Delta\Psi_m$ mitochondrial respiration rate was lower at 15°C compared with 37°C. We then applied the elasticity analysis described above to quantitatively examine how temperature affected respiration of mitochondria from both normothermic

Table 2. *Summary of the top-down elasticity analysis conducted in this study*

	Normothermia, 37°C		Normothermia, 15°C		Torpor, 37°C		Torpor, 15°C	
	State 3	*State 4*	*State 3*	*State 4*	*State 3*	*State 4*	*State 3*	*State 4*
				Flux control coefficients				
C_c^{JO2}	0.82	0.5	0.82	0.66	0.8	0.56	0.76	0.34
C_l^{JO2}	0.01	0.5	0.01	0.34	0.02	0.44	0.1	0.66
C_p^{JO2}	0.16		0.16		0.18		0.14	
				Elasticity coefficients				
$\varepsilon^c_{\Delta P}$	−2.4	−14	−1.5	−7	−2.2	−9.3	−3.9	−12.6
$\varepsilon^l_{\Delta P}$	0.62	14.3	0.22	13.5	1.2	11.9	1.3	6.5
$\varepsilon^p_{\Delta P}$	12.1		7.3		9.9		19.8	

	N37 to T37		N37 to N15		T37 to T15	
	State 3	*State 4*	*State 3*	*State 4*	*State 3*	*State 4*
			Integrated elasticity coefficients			
$IE^c_{\Delta q}$	−0.37	−0.63	−1.15	−1.45	−0.81	−1.69
$IE^l_{\Delta q}$	0.03	0.6	−0.68	−0.07	−0.09	0.32
$IE^p_{\Delta q}$	0.02		0.76		−1.01	
			Partial integrated response coefficients			
${}^cIR^{JO2}_{\Delta q}$	−0.3	−0.31	−0.94	−0.73	−0.64	−0.95
${}^lIR^{JO2}_{\Delta q}$	0	0.3	0	−0.03	0	0.14
${}^pIR^{JO2}_{\Delta q}$	0		0.12		−0.18	
IR	−0.3	−0.01	−0.82	−0.76	−0.82	−0.81

Flux control coefficients and elasticity coefficients for *state 3* and *state 4* are presented for each metabolic state at both 37°C and 15°C, and integrated elasticity coefficients and partial integrated response coefficients are presented for the transition from normothermia to torpor (at 37°C) and for the effect of a reduction in temperature (37°C to 15°C) for both normothermic and torpid animals. C, control; c, substrate oxidation; l, proton leak; p, phosphorylation; JO2, mitochondrial respiration rate; ΔP, proton motive force; IE, integrated elasticity; IR, integrated response; Δq, change in condition (from normothermy to torpor, or from 37°C to 15°C).

and torpid animals (Table 2). For mitochondria from both normothermic and torpid animals, *state 3* respiration rate was reduced by 82% at 15°C compared with 37°C, but there was a difference in how this temperature-induced reduction of respiration was achieved between the metabolic states. For mitochondria from normothermic animals, there was a considerable temperature-induced decrease in substrate oxidation capacity that was partially offset by a small increase in phosphorylation capacity. By contrast, for mitochondria from torpid animals, the reduction of *state 3* respiration was achieved by a less pronounced reduction of substrate oxidation capacity and a temperature-induced reduction of phosphorylation capacity. *State 4* respiration rate was also reduced by temperature to a similar extent in mitochondria from both normothermic and torpid animals (~80%), but, once again, the temperature-dependant mechanism differed between metabolic states. For normothermic mitochondria, *state 4* respiration was predominantly reduced by the considerable reduction of substrate oxidation capacity, whereas for torpid mitochondria, there was an even more pronounced reduction of substrate oxidation capacity, but its effects on respiration were partially counteracted by a temperature-induced increased in proton leakiness of the IMM. Fig. 8 summarizes the contribution of each component of OxPhos to the changes in mitochondrial respiration between metabolic states and/or temperatures, based on partial integrated response coefficients.

DISCUSSION

To our knowledge, this study represents the first investigation of mitochondrial respiration for a daily heterotherm, and it is also the first study to simultaneously examine the role of both active regulated changes and passive thermal effects during torpor to the extent of determining how each affects OxPhos to bring about a reduction of mitochondrial respiration. We have demonstrated active regulated changes of liver mitochondrial metabolism during daily torpor, involving a reduced substrate oxidation capacity (likely upstream of complex III) and an increased proton conductance. Additionally, we have shown that mitochondrial respiration is also reduced by passive thermal effects during torpor through changes to all components of OxPhos. Overall, these active and passive changes reduce liver mitochondrial respiration considerably during daily torpor and likely contribute significantly to the reduction of MR.

At 37°C, *state 3* respiration, but not *state 4* respiration, was reduced in mitochondria from torpid animals. These data suggest that liver mitochondrial respiration is actively downregulated during torpor. However, *state 3* respiration was only reduced by 30%. This is considerably less than the degree of active suppression of *state 3* respiration in liver mitochondria during hibernation, which has been reported to be 55–72% for succinate oxidation (3, 20, 50, 52). This is consistent with the more moderate reduction of MR during daily torpor. At 15°C, respiration of both *states 3* and *4* was reduced 75–82% compared with 37°C, which shows that passive thermal effects also play an important role in the reduction of liver mitochondrial respiration during daily torpor. When mitochondrial respiration from torpid animals at 15°C is compared with mitochondrial respiration from normothermic animals at 37°C, which approximates the in vivo reduction of mitochondrial metabolism

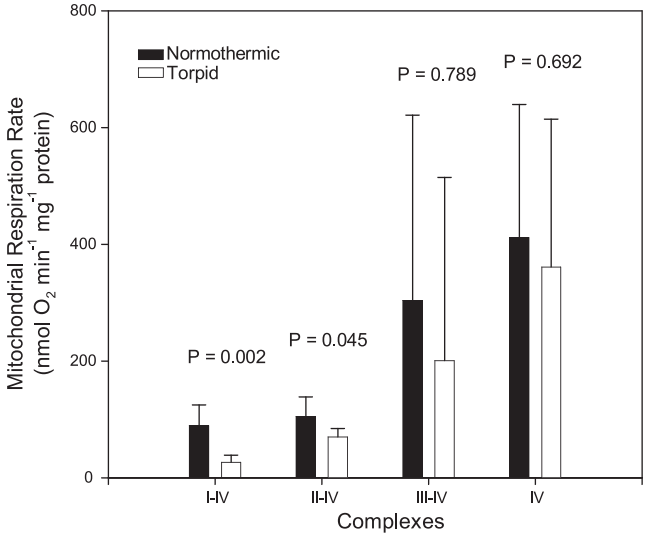

Fig. 6. Comparison of flux through different complexes of the electron transport chain in liver mitochondria isolated from normothermic and torpid animals. Flux through complexes I–IV and II–IV were significantly reduced in mitochondria from torpid animals, whereas flux through complex III-IV and complex IV were not significantly different between the metabolic states. *P* values are from Student's *t*-test; $n = 12$ for normothermia and $n = 5$ for torpor, except for complex III-IV, where $n = 8$ and $n = 4$ for normothermia and torpor, respectively. Values are means ± SD.

during torpor, respiration of *states 3* and *4* was reduced by 88% and 81%, respectively. If liver respiration represents 12–17% of MR (49), then the reduction of liver mitochondrial respiration observed in this study could account for up to 15% of the reduction of MR during torpor. Since MR is reduced by 65% during daily torpor in this species (25), the reduction of liver mitochondrial metabolism may be responsible for 15–23% of the energy savings during torpor. At the same time, since liver mitochondrial density was not different between normothermic and torpid animals, based on citrate synthase activity, it would seem that differences in liver mitochondrial respiration rates between normothermic and torpid animals are not compensated for by differences in total mitochondria.

As mentioned, there was no difference in respiration rates of *states 3* or *4* between normothermic and torpid animals at 15°C. Two studies involving the hibernating ground squirrel, *Spermophillus tridecemlineatus*, have shown a similar result (52; Gerson AR, Brown JCL, Staples JF, unpublished observation), an inhibition in liver mitochondria was observed at 37°C, but not at lower temperatures, although there is a study on hibernation in which an active inhibition has been demonstrated even at low temperatures (55). Based on the results from our study and the two studies of hibernating ground squirrels, it would seem that a torpid animal could reduce liver mitochondrial respiration to its torpid rate simply by allowing T_b to decline. This likely explains why whole animal Q_{10} measurements for daily heterotherms have been calculated to be <3, which are within the range commonly attributed to passive temperature effects, even though there is evidence of active inhibition. In our study, Q_{10} was 2.64 and 2.13 for *states 3* and *4*, respectively. Therefore, we propose that the active changes may reduce oxygen consumption (and MR) during torpor, while T_b remains high (i.e., during entrance, and torpor at thermoneutrality), whereas passive thermal effects may predominate at lower T_b.

Our kinetic analysis showed that the active reduction of *state 3* respiration was brought about by a reduction of substrate oxidation capacity, not by any change in phosphorylation capacity. Our analysis also showed that, in liver mitochondria from the dwarf Siberian hamster, substrate oxidation has 76–82% control over *state 3* respiration, which is more than has been previously reported for rat liver mitochondria (60–80%) (5, 18, 48). Several studies of mitochondrial respiration in hibernators have shown that the substrate oxidation capacity is reduced in the torpid state and have implicated the ETC as the site of this inhibition. Complex II was inhibited during hibernation in Arctic ground squirrels (20), whereas the ubiquinone pool and/or complex III was inhibited in Richardson's ground squirrels (11). Furthermore, a study of 13-lined ground squirrels showed that complex IV was inhibited during hibernation, although it was not likely responsible for the depressed mitochondrial respiration since it was also inhibited during arousal when mitochondrial respiration was high, and, additionally, there was an inhibition between complexes II and IV (52). Therefore, studies of liver mitochondrial respiration during hibernation in ground squirrels suggest that an inhibition of

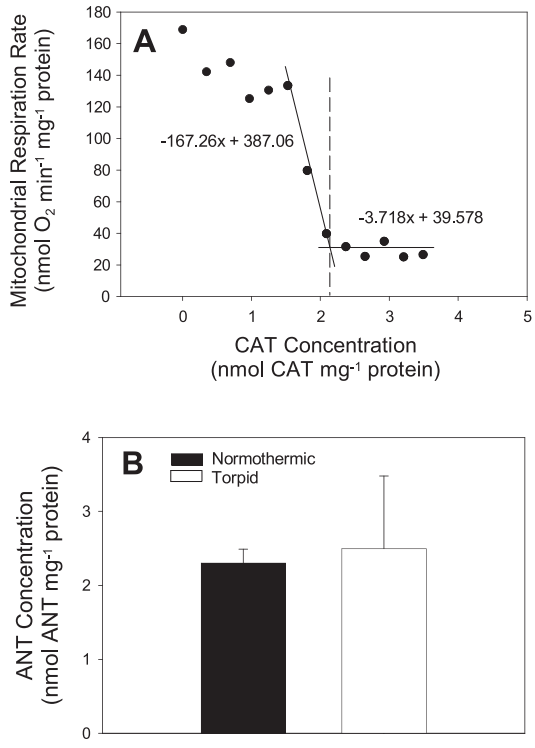

Fig. 7. The adenine nucleotide translocator (ANT) is not responsible for the change in proton conductance during daily torpor. *A*: concentration of ANT was determined by titrating *state 3* mitochondrial respiration with carboxyatractyloside (CAT), a noncompetitive inhibitor of ANT. The concentration of ANT is determined by the intersection of the line of maximal slope and the essentially horizontal line that results from continued titration once ANT is fully inhibited. The concentration of CAT at which these 2 lines intersects represents the concentration of CAT required to fully reduce *state 3* respiration to *state 4* respiration, and, because the binding of CAT to ANT is essentially stoichiometric, represents the concentration of ANT in the mitochondrial preparation. *B*: concentration of ANT did not differ ($P = 0.78$, Student's *t*-test, $n = 10$ for normothermia and $n = 4$ for torpor) between normothermia and torpor. Values are means ± SD.

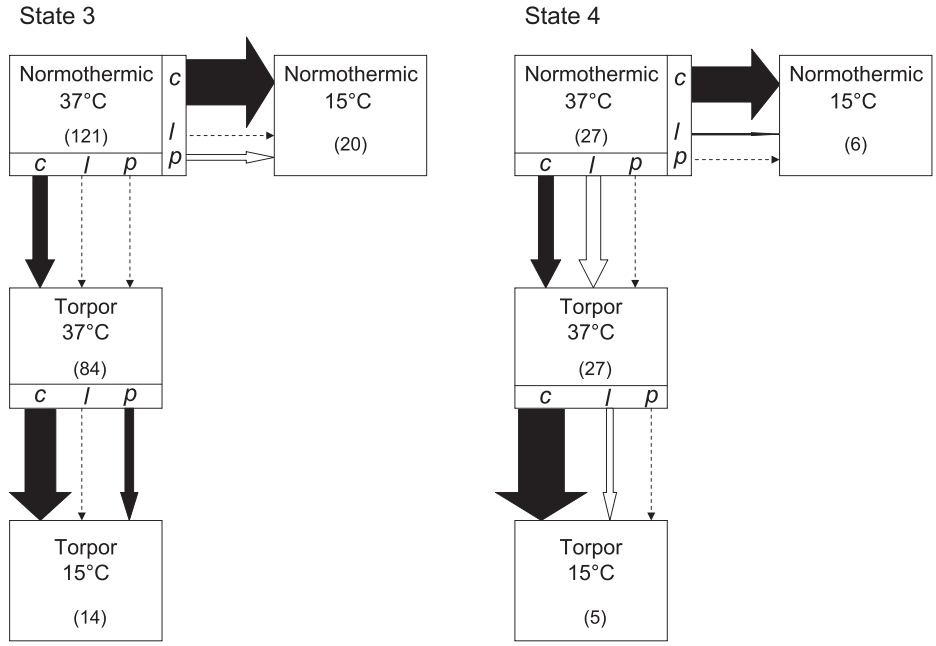

Fig. 8. Partially integrated response coefficients calculated for each component of oxidative phosphorylation can be used to show which components of oxidative phosphorylation (OxPhos) contribute to a change in *state 3* and *state 4* mitochodrial respiration in response to an effector, such as torpor or temperature. Each box represents a combination of metabolic state and temperature, and the number in parentheses within each box is the mitochondrial respiration rate (in nmol $O_2 \cdot min^{-1} \cdot mg\ protein^{-1}$). Arrows between boxes represent the partial integrated response coefficients for each component of OxPhos. The letter adjacent to an arrow indicates the component that the arrow represents (by convention: *c*, substrate oxidation; *l*, proton leak; *p*, phosphorylation), and the size of the arrow indicates the relative magnitude of the partial integrated response coefficient. Filled arrows and open arrows represent negative and positive partial integrated response coefficients, respectively, whereas dashed arrows represent zero values. For *state 3*, the decrease in respiration rate for the transition from normothermia to torpor at 37°C resulted entirely from a decrease in substrate oxidation. The further decrease in respiration rate for torpid mitochondria for the transition from 37°C to 15°C was brought about by a decrease in both substrate oxidation and phosphorylation. By comparison, the decrease in respiration rate for normothermic mitochondria for the same temperature transition resulted from a greater decrease in substrate oxidation but a small increase in phosphorylation. For *state 4*, there was no change in mitochondrial respiration rate upon the transition from normothermia to torpor because substrate oxidation decreased but proton leakiness increased correspondingly. The respiration rate of mitochondria isolated from torpid animals did decrease during the transition from 37°C to 15°C, mostly because of a large decrease in substrate oxidation, although there was a small increase in proton leakiness. By contrast, the respiration rate of mitochondria isolated from normothermic animals decreased upon transition from 37°C to 15°C because of a considerable decrease in substrate oxidation and small decrease in proton leakiness.

the ETC likely occurs during torpor, involving the middle segment of the chain.

To determine whether the site of inhibition is similar during daily torpor, we decided to further investigate the active inhibition of substrate oxidation. Compared with mitochondria from normothermic animals, *state 3* respiration at 37°C on glutamate (a complex I-linked substrate) and succinate (a complex II-linked substrate) were significantly reduced, whereas respiration on decylubiquinol (a complex III-linked substrate) and TMPD (a complex IV-linked substrate) were not reduced in mitochondria from torpid animals. The reduced respiration on glutamate does not likely involve a reduction in the activity of glutamate dehydrogenase since this enzyme has been shown to undergo no change in activity during daily torpor in dwarf Siberian hamsters (36). These data suggest that the inhibition of the substrate oxidation component is upstream of complex III, and either of three possible mechanisms could explain the results of our study: *1*) each dehydrogenase (complex I and complex II) is downregulated independently, to a different extent; *2*) complex I and the ubiquinone pool are downregulated, but not complex II; or *3*) the glutamate and dicarboxylate transporters are downregulated.

To determine the possible role of the first two mechanisms, we investigated the maximal activity of complex I and complex II-III in isolated mitochondria, but there was no difference between normothermic and torpid animals. This does not preclude the possible inhibition of this portion of the ETC by some mechanism(s) which was subsequently removed during our homogenization and assay, but does suggest the mechanism does not involve reduced levels of the enzyme complexes. Little is known about the regulation of complex I (25, 54), but complex II is known to be inhibited by oxaloacetate (28), which may downregulate mitochondrial respiration in hibernation (20). The glutamate (both glutamate/aspartate and glutamate/OH^-) and dicarboxylate transporters transport glutamate and succinate/malate, respectively. In particular, the dicarboxylate transporter has been shown to have considerable control over *state 3* respiration in rats (26) and may be a site of inhibition during torpor. The ubiquinone pool has also been implicated as a possible site of inhibition of substrate oxidation during hibernation, although it does not likely involve a reduction of ubiquinone content during hibernation in ground squirrels (23), but this remains to be demonstrated in daily heterotherms. It is possible that changes in mitochondrial matrix volume have some role in regulating mitochondrial metabolism during daily torpor, since reductions in matrix volume have been shown to reduce oxidation of NADH-producing substrates and succinate but not duroquinol or TMPD in rats (31), and changes in matrix volume may contribute to reductions in mitochondrial respiration in hibernators (11), but this has not

yet been investigated for daily heterotherms. Therefore, although we have demonstrated the ETC is likely inhibited upstream of complex III, we have not been able to further elucidate the mechanism of inhibition.

Although we have shown that phosphorylation kinetics were unaltered during daily torpor, our analysis only considered the mitochondrial components of phosphorylation (such as ATP synthase, ANT, phosphate transporter) and disregarded other cellular components (such as various ATPases). The ATP-consuming processes of transcription and translation are actively reduced during torpor in dwarf Siberian hamsters (17), and so it may be that active regulated changes to the phosphorylation component predominantly involve extramitochondrial modifications. On this basis, in vivo, *state 3* respiration may be actively reduced by >30%, and so energy savings during entrance and/or torpor at thermoneutrality may be greater than this present study alone would predict. At the same time, however, it seems unlikely that mitochondria would operate at *state 3* during torpor given that many ATP-consuming processes are downregulated during torpor in both daily heterotherms and hibernators [e.g., transcription/translation, (17, 22), Na^+-K^+-ATPase, (47)], and so the effect of an active reduction of *state 3* respiration on MR during torpor may be somewhat less than predicted. It should also be noted that the lack of difference in ANT concentration between normothermia and torpor is consistent with our observation that phosphorylation kinetics were unchanged during the transition to daily torpor.

In contrast to *state 3* respiration, *state 4* respiration was not actively reduced during daily torpor. This absence of a reduction of *state 4* respiration is interesting since *state 4* respiration has been shown to be actively reduced (when measured at 37°C) in hibernation (3, 55). Our analysis demonstrated that the lack of reduction of *state 4* respiration, despite a reduction of substrate oxidation capacity, occurred because IMM proton leakiness was simultaneously increased. Proton leak has often been considered an inefficiency of mitochondrial metabolism, and, on this basis, many studies of hypometabolic states have predicted that the proton conductance of the IMM might be reduced to reduce oxygen consumption and conserve energy. However, this prediction has neglected that *1*) proton leak depends upon the translocation of protons via substrate oxidation and *2*) proton leak may have benefits as well as costs. Notwithstanding, data from our lab demonstrate reduced proton leakiness in mammalian hibernation (Gerson AR, Brown JCL, Staples JF, unpublished observation), although another study suggested that there is no significant change in the membrane conductance in hibernation although there was a trend toward decreased leakiness (3). Additionally, studies of hypometabolic states in nonmammalian organisms, such as frogs (65) and snails (4), have also shown that proton conductance is unaltered.

In the present study, however, the proton leakiness of mitochondria from animals during daily torpor was increased, both actively and passive, compared to normothermic animals, yet *state 4* respiration did not differ at either assay temperature. The reason for this lack of difference in respiration rate despite considerable differences in proton leakiness is that substrate oxidation capacity was drastically reduced in both metabolic states; that is to say, the ETC did not increase its activity to replace the protons that were leaking through the membrane, and so respiration rate did not increase. Therefore, there seems to be no increased energetic cost, at least in terms of mitochondrial oxygen consumption rate, associated with an increased IMM leakiness during torpor. At the same time, proton leakiness has considerably less control over *state 4* respiration in liver mitochondria from dwarf Siberian hamsters (34–66%) compared with rat liver mitochondria (70–90%) (18, 32), which may also contribute to the lack of effect of increased proton leakiness on *state 4* respiration rate. Moreover, it is possible that the active increase in IMM proton leakiness allows daily heterotherms to take advantage of the benefits of proton leakiness, such as increased heat production during arousal or reduced reactive oxygen species (ROS) production during torpor and/or arousal (59), without paying a significant energetic cost. While these benefits of increased proton conductance could also be advantageous during normothermy, because substrate oxidation capacity is higher, the associated costs in terms of substrate utilization might be prohibitive.

Although we have attributed differences in the proton leak kinetics to a difference in IMM proton conductance, there are two other possible interpretations that must be considered, including changes in *1*) redox slip and/or *2*) ROS production. Redox slip occurs when electrons are flowing through the ETC but protons are not being translocated (56); it results in electron flow which contributes to oxygen consumption without contributing to the generation of ΔP (i.e., higher levels of mitochondrial respiration at a given value of $\Delta\Psi_m$). Evidence of redox slip is equivocal (5), however, and an examination of the effects of torpor on redox slip were beyond the scope of this study. ROS are produced when electrons leave the ETC prematurely and univalently reduce oxygen to superoxide anions, rather than water. Therefore, changes in ROS production may have the same effect as changes in proton leakiness, that is, to reduce ΔP without reducing oxygen consumption. However, increased ROS production of mitochondria from torpid animals is not likely sufficient to explain the difference in proton leak kinetics observed in our study. ROS production is thought to account for no more than 5% of total mitochondrial oxygen consumption (13), and so ROS production would have to increase at least eightfold to explain the 40% increase in proton leak kinetics observed in this study. Therefore, the observed difference in proton leak likely represents an increase in IMM proton conductance. Nonetheless ROS production is thought to increase during arousal (68), and we plan to compare rates of ROS production between normothermia, torpor, and arousal.

Our study did not answer how the leakiness of the IMM is increased during daily torpor. There are several potential mechanisms that can alter membrane proton permeability, including changes in membrane surface area and/or changes in membrane phospholipid fatty acid composition (7) and changes in the concentration of ANT (9). The concentration of ANT did not change during daily torpor and, therefore, cannot explain our observed increase in IMM leakiness. We plan to explore the possible role of IMM remodeling, by examining differences in phospholipid head group and fatty acyl composition between normothermia and torpor.

In addition to active regulated changes, we have shown that passive thermal effects also contribute to the reduction of mitochondrial respiration during daily torpor, and our analysis has shown that this reduction is predominantly achieved through a temperature-dependent reduction of substrate oxidation capacity. A drop in temperature from 37°C to 15°C reduced substrate oxidation considerably in mitochondria from

both normothermic and torpid animals, but its effects on the other components of OxPhos was dependent on metabolic state. Reduced temperature decreased the phosphorylation capacity of mitochondria from torpid animals but increased the capacity of phosphorylation of mitochondria from normothermic animals. Similarly, reduced temperature decreased the IMM proton leakiness of mitochondria from normothermic animals but increased proton conductance of mitochondria from torpid animals. Generally, these differential thermal responses of phosphorylation and proton leakiness did not have substantial effects on the extent of temperature-dependent changes in mitochondrial respiration compared with the effects of temperature on substrate oxidation. Regardless, we are interested in examining changes in mitochondrial membrane composition because it may explain why temperature had different effects on these components of OxPhos in normothermic and torpid mitochondria. The differential temperature sensitivity of the phosphorylation and proton leak component in mitochondria from torpid and normothermic animals may be a passive result of the alterations of the membrane properties, which increased proton conductance, since it has been shown that the nature of membranes can influence the activity of some intermembrane proteins, such as the sodium-potassium pump (72).

At the time of sampling, the torpid animals used in this study had a 23% lower body weight than the normothermic animals. Therefore, it could be suggested that the differences observed in this study are attributable to differences in body weight rather than differences in metabolic state. To assess this possibility, we conducted an analysis of covariance to determine whether *state 3* respiration was different between torpor and normothermia even when body mass was considered. Our analysis demonstrated that body mass had no significant effect on *state 3* respiration ($F_{1/17} = 1.841$, $P = 0.19$). At the same time, an inverse relationship between body mass and proton leakiness has been demonstrated in mammals (57); however, using the allometric equation for this relationship, we can demonstrate that the lower body mass of the torpid animals could only account for, at most, a 4% increase in proton leakiness, which is considerably less than the observed increase (~40%) during daily torpor in this study.

Perspectives and Significance

The reduction of MR which occurs during daily torpor is well characterized, but the mechanisms by which this reduction is achieved have been poorly understood. Additionally, the mechanisms by which spontaneous daily torpor is induced are still not fully comprehended. The findings of the present study make an important contribution to our understanding of how MR is reduced during daily torpor by demonstrating that active regulated changes to substrate oxidation are involved, likely upstream of complex III. In future, we hope to determine the exact site of this decrease in substrate oxidation because this information could form the basis of a bottom-up approach to understanding how daily torpor is induced at higher levels of organization. Moreover, our study has shown that, contrary to our expectations, IMM proton leakiness was increased during daily torpor, and we have proposed that this leakier membrane may play a role in reducing ROS production during torpor. We hope to explore both the nature of the changes to IMM proton leakiness and to determine their effect on ROS production. Furthermore, by comparing the findings of the present study to similar studies in hibernators, we may be able to better understand whether these two hypometabolic states are evolutionarily related. Many studies have compared hibernation and daily torpor at the whole animal level (in terms of MR and T_b), and these studies have suggested that hibernation and daily torpor are similar phenomena, except that the metabolic suppression is longer and deeper in hibernation. Fewer studies have compared these two states at the biochemical and physiological level but have also shown similarities between hibernation and daily torpor, such as downregulation of pyruvate dehydrogenase activity, suppression of protein synthesis, and a switch to fatty acid metabolism. Our findings suggest that daily torpor and hibernation also exhibit physiological distinctions, however, since IMM proton leakiness has been shown to remain unchanged or be reduced during hibernation, contrary to our findings for daily torpor.

ACKNOWLEDGMENTS

We thank the veterinary technicians of the Animal Care and Veterinary Services Department of the University of Western Ontario for their gracious assistance with the surgical supplies. Also, we thank Tyler Done and Sally Ngai for excellent assistance with surgeries and animal care. The preliminary studies of Cheryl Schaefer and Erin Koen helped to refine the current experimental design. Comments from anonymous reviewers helped to improve this paper.

GRANTS

Financial support for this research came in the form of Discovery and Research Tools and Infrastructure Grants (to J. F. Staples) and a Postgraduate Scholarship (to J. C. L. Brown) from the Natural Sciences and Engineering Research Council of Canada.

REFERENCES

1. **Ainscow EK, Brand MD.** The responses of rat hepatocytes to glucagon and adrenaline: application of quantified elasticity analysis. *Eur J Biochem* 265: 1043–1055, 1999.
2. **Arnold W.** Social thermoregulation during hibernation in alpine marmots (*Marmota marmota*). *J Comp Physiol [B]* 158: 151–156, 1988.
3. **Barger JL, Brand MD, Barnes BM, Boyer BB.** Tissue-specific depression of mitochondrial proton leak and substrate oxidation in hibernating arctic ground squirrels. *Am J Physiol Regul Integr Comp Physiol* 284: R1306–R1313, 2003.
4. **Bishop T, St-Pierre J, Brand MD.** Primary causes of decreased mitochondrial oxygen consumption during metabolic depression in snail cells. *Am J Physiol Regul Integr Comp Physiol* 282: R372–R382, 2002.
5. **Brand MD, Harper ME, Taylor HC.** Control of the effective P/O ratio of oxidative phosphorylation in liver mitochondria and hepatocytes. *Biochem J* 291: 739–748, 1993.
6. **Brand MD, Chien LF, Diolez P.** Experimental discrimination between proton leak and redox slip during mitochondrial electron transport. *Biochem J* 297: 27–29, 1994.
7. **Brand MD, Chien LF, Ainscow EK, Rolfe DFS, Porter RK.** The causes and functions of mitochondrial proton leak. *Biochim Biophys Acta* 1187: 132–139, 1994.
8. **Brand MD.** Top-down elasticity analysis and its application to energy metabolism in isolated mitochondria and intact cells. *Mol Cell Biochem* 184: 13–20, 1998.
9. **Brand MD, Pakay JL, Ocloo A, Kokoszka J, Wallace DC, Brookes PS.** The basal proton conductance of mitochondria depends on adenine nucleotide translocase content. *Biochem J* 392: 353–362, 2005.
10. **Brookes PS.** Mitochondrial H^+ leak and ROS generation: an odd couple. *Free Radic Biol Med* 38: 12–23, 2005.
11. **Brustovetsky NN, Amerkhanov ZG, Popova EY, Konstantinov AA.** Reversible inhibition of electron transfer in the ubiquinol cytochrome *c* reductase segment of the mitochondrial respiratory chain in hibernating ground squirrels. *FEBS Lett* 263: 73–76, 1990.
12. **Buttgereit F, Grant A, Muller M.** The effects of methylprednisolone on oxidative phosphorylation in concanavalin-A-stimulated thymocytes: top

down elasticity analysis and control analysis. *Eur J Biochem* 223: 513–519, 1994.
13. **Cadenas E.** Biochemistry of oxygen toxicity. *Annu Rev Biochem* 58: 79–110, 1989.
14. **Chamberlin ME.** Top-down control analysis of the effect of temperature on ectotherm oxidative phosphorylation. *Am J Physiol Regul Integr Comp Physiol* 287: R794–R800, 2004.
15. **Dark J, Miller DR, Licht P, Zucker I.** Glucoprivation counteracts effects of testosterone on daily torpor in Siberian hamsters. *Am J Physiol Regul Integr Comp Physiol* 270: R398–R403, 1996.
16. **Demura M, Kamo N, Kobatake Y.** Binding of lipophilic cations to the liposomal membrane: thermodynamic analysis. *Biochim Biophys Acta* 903: 303–308, 1987.
17. **Diaz MB, Lange M, Heldmaier G, Klingenspor M.** Depression of transcription and translation during daily torpor in the Djungarian hamster (*Phodopus sungorus*). *J Comp Physiol [B]* 174: 495–502, 2004.
18. **Dufour S, Rousse N, Canioni P, Diolez P.** Top-down control analysis of temperature effect on oxidative phosphorylation. *Biochem J* 314: 743–751, 1996.
19. **Duong CA, Sepulveda CA, Graham JB, Dickson KA.** Mitochondrial proton leak rates in the slow, oxidative myotomal muscle and liver of the endothermic shortfin mako shark (*Isurus oxyrinchus*) and the ectothermic blue shark (*Prionace glauca*) and leopard shark (*Triakis semifasciata*). *J Exp Biol* 209: 2678–2685, 2006.
20. **Fedotcheva NJ, Sharyshev AA, Mironova GD, Kondrashova MN.** Inhibition of succinate oxidation and K^+ transport in mitochondria during hibernation. *Comp Biochem Physiol B* 82: 191–195, 1985.
21. **Florant GL, Heller HC.** CNS regulation of body temperature in euthermic and hibernating marmots (*Marmota flaviventris*). *Am J Physiol Regul Integr Comp Physiol* 232: R203–R208, 1977.
22. **Frerichs KU, Smith CB, Brenner M, DeGracia DJ, Krause GS, Marrone L, Dever TE, Hallenbeck JM.** Suppression of protein synthesis in brain during hibernation involves inhibition of protein initiation and elongation. *Proc Natl Acad Sci USA* 95: 14511–14516, 1998.
23. **Gehnrich SC, Aprille JR.** Hepatic gluconeogenesis and mitochondrial function during hibernation. *Comp Biochem Physiol B* 91: 11–16, 1988.
24. **Geiser F.** Metabolic rate and body temperature reduction during hibernation and daily torpor. *Annu Rev Physiol* 66: 239–274, 2004.
25. **Grivennikova VG, Kapustin AN, Vinogradov AD.** Catalytic activity of NADH-ubiquinone oxidoreductase (complex I) in intact mitochondria: evidence for the slow active/deactive transition. *J Biol Chem* 276: 9038–9044, 2001.
26. **Groen AK, Wanders RJA, Westerhoff HV, van der Meer R, Tager JM.** Quantification of the contribution of various steps to the control of mitochondrial respiration. *J Biol Chem* 257: 2754–2757, 1982.
27. **Guderley H, Turner N, Else PL, Hulbert AJ.** Why are some mitochondria more powerful than others: insights from comparisons of muscle mitochondria from three terrestrial vertebrates. *Comp Biochem Physiol B* 142: 172–180, 2005.
28. **Gutman M.** Modulation of mitochondrial succinate dehydrogenase activity, mechanism and function. *Mol Cell Biochem* 20: 41–60, 1978.
29. **Guppy M, Withers P.** Metabolic depression in animals: physiological perspectives and biochemical generalizations. *Biol Rev* 74: 1–40, 1999.
30. **Hafner RP, Brown GC, Brand MD.** Analysis of the control of respiration rate, phosphorylation rate, proton leak rate and protonmotive force in isolated mitochondria using the "top-down" approach of metabolic control theory. *Eur J Biochem* 188: 313–319, 1990.
31. **Halestrap AP.** The regulation of the matrix volume of mammalian mitochondria in vivo and in vitro and its role in the control of mitochondrial metabolism. *Biochim Biophys Acta* 973: 335–382, 1989.
32. **Harper ME, Brand MD.** The quantitative contributions of mitochondrial proton leak and ATP turnover reactions to the changed respiration rates of hepatocytes from rats of different thyroid status. *J Biol Chem* 268: 14850–14860, 1993.
33. **Harper ME, Brand MD.** Use of top-down elasticity analysis to identify sites of thyroid hormone-induced thermogenesis. *Proc Soc Exp Biol Med* 208: 228–237, 1995.
34. **Heldmaier G, Steinlechner S.** Seasonal pattern and energetics of short daily torpor in the Djungarian hamster, *Phodopus sungorus*. *Oecologia* 48: 265–270, 1981.
35. **Heldmaier G, Ruf T.** Body temperature and metabolic rate during natural hypothermia in endotherms. *J Comp Physiol [B]* 162: 696–706, 1992.
36. **Heldmaier G, Klingenspor M, Werneyer M, Lampi BJ, Brooks SPJ, Storey KB.** Metabolic adjustments during daily torpor in the Djungarian hamster. *Am J Physiol Endocrinol Metab* 276: E896–E906, 1999.
37. **Heldmaier G, Elvert R.**How to enter torpor: thermodynamic and physiological mechanisms of metabolic depression. In: *Life in the Cold: Evolution, Mechanisms, Adaptations,*and*Application*, edited by Barnes BM, Carey HV. Fairbanks, AK: University of Alaska Press, 2004.
38. **Hiebert SM, Fulkerson EK, Lindermayer KT, McClure SD.** Effect of temperature on preference for dietary unsaturated fatty acids in the Djungarian hamster (*Phodopus sungorus*). *Can J Zool* 78: 1361–1368, 2000.
39. **Humphries MM, Thomas DW, Kramer DL.** The role of energy availability in mammalian hibernation: a cost-benefit approach. *Physiol Biochem Zool* 76: 165–179, 2003.
40. **Hwang YT, Larivière S, Messier F.**Energetic consequences and ecological significance of heterothermy and social thermoregulation in striped skunks (*Mephitis mephitis*). *Physiol Biochem Zool* 80: 138–145.
41. **Jefimow M, Wojciechowski M, Masuda A, Oishi T.** Correlation between torpor frequency and capacity for nonshivering thermogenesis in the Siberian hamster (*Phodopus sungorus*). *J Therm Biol* 29: 641–647, 2004.
42. **Kayser EB, Sedensky MM, Morgan PG, Hoppel CL.** Mitochondrial oxidative phosphorylation is defective in the long-lived mutant clk-1. *J Biol Chem* 279: 54479–54486, 2004.
43. **Kemp TS.** The origin of mammalian endothermy: a paradigm for the evolution of complex biological structure. *Zool J Linnean Soc* 147: 473–488, 2006.
44. **Lombardi A, Lanni A, Moreno M, Brand MD, Goglia F.** Effect of 3,5-di-iodo-L-thyronine on the mitochondrial energy-transduction apparatus. *Biochem J* 330: 521–526, 1998.
45. **Lyman CP, O'Brien RC, Greene GC, Papafrangos ED.** Hibernation and longevity in the Turkish hamster, *Mesocricetus brandti*. *Science* 212: 668–670, 1981.
46. **Lyman CP, Willis JS, Malan A, Wang LCH.** *Hibernation* and *torpor in mammals* and *birds*. New York: Academic, 1982.
47. **MacDonald JA, Storey KB.** Regulation of ground squirrel Na^+K^+-ATPase activity by reversible phosphorylation in hibernation. *Biochem Biophys Res Commun* 254: 424–429, 1999.
48. **Marcinkeviciute A, Mildaziene V, Crumm S, Demin O, Hoek JB, Kholodenko B.** Kinetics and control of oxidative phosphorylation in rat liver mitochondria after chronic ethanol feeding. *Biochem J* 349: 519–526, 2000.
49. **Martin AW, Fuhrman FA.** The relationship between summated tissue respiration and metabolic rate in the mouse and dog. *Physiol Zool* 28: 18–34, 1955.
50. **Martin SM, Maniero GD, Carey C, Hand SC.** Reversible depression of oxygen consumption in isolated liver mitochondria during hibernation. *Physiol Biochem Zool* 72: 255–264, 1999.
51. **Mildaziene V, Nauciene Z, Baniene R, Grigiene J.** Multiple effects of 2,2′,5,5′-tetrachlorobiphenyl on oxidative phosphorylation in rat liver mitochondria. *Toxicol Sci* 65: 220–227, 2002.
52. **Muleme HM, Walpole AC, Staples JF.** Mitochondrial metabolism in hibernation: metabolic suppression, temperature effects, and substrate preferences. *Physiol Biochem Zool* 79: 474–483, 2006.
53. **Ortmann S, Heldmaier G.** Regulation of body temperature and energy requirements of hibernating Alpine marmots (*Marmota marmota*). *Am J Physiol Regul Integr Comp Physiol* 278: R698–R704, 2000.
54. **Papa S, Sardanelli AM, Scacco S, Petruzzella V, Technikova-Dobrova Z, Vergari R, Signorile A.** The NADH: ubiquinone oxidoreductase (complex I) of the mammalian respiratory chain and the cAMP cascade. *J Bioenerg Biomembr* 34: 1–10, 2002.
55. **Pehowich DJ, Wang LCH.** Seasonal changes in mitochondrial succinate dehydrogenase activity in a hibernator, *Spermophilus richardsonii*. *J Comp Physiol [B]* 154: 495–501, 1984.
56. **Pietrobon D, Azzone GF, Walz D.** Effect of funiculoson and antimycin A on the redox-driven H^+-pumps in mitochondria: on the nature of "leaks". *Eur J Biochem* 117: 389–394, 1981.
57. **Porter RK, Hulbert AJ, Brand MD.** Allometry of mitochondria proton leak: influence of membrane surface area and fatty acid composition. *Am J Physiol Regul Integr Comp Physiol* 271: R1550–R1560, 1996.
58. **Reynafarje B, Costa LE, Lehninger AL.** O_2 solubility in aqueous media determined by a kinetic method. *Anal Biochem* 145: 406–418, 1985.
59. **Rolfe DFS, Brand MD.** The physiological significance of mitochondrial proton leak in animal cells and tissues. *Biosci Rep* 17: 9–16, 1997.

60. **Rolfe DFS, Hulbert AJ, Brand MD.** Characteristics of mitochondrial proton leak and control of oxidative phosphorylation in the major oxygen-consuming tissues of the rat. *Biochim Biophys Acta* 1188: 405–416, 1994.
61. **Rolfe DFS, Brown GC.** Cellular energy utilization and molecular origin of standard metabolic rate in mammals. *Physiol Rev* 77: 731–758, 1997.
62. **Rottenberg H.** Metabolic potential and surface potential in mitochondria: uptake and binding of lipophilic cations. *J Membr Biol* 81: 127–138, 1984.
63. **Snyder GK, Nestler JR.** Relationships between body temperature, thermal conductance, Q_{10} and energy metabolism during daily torpor and hibernation in rodents. *J Comp Physiol [B]* 159: 667–675, 1990.
64. **Stahl WR.** Organ weights in primates and other mammals. *Science* 150: 1039–1042, 1965.
65. **St-Pierre J, Brand MD, Boutilier RG.** The effect of metabolic depression on proton leak rate in mitochondria from hibernating frogs. *J Exp Biol* 203: 1469–1476, 2000.
66. **Sutherland BA, Shaw OM, Clarkson AN, Jackson DM, Sammut IA, Appleton I.** Neuroprotective effects of (−)-epigallocatechin gallate after hypoxia-ischemia-induced brain damage: novel mechanisms of action. *FASEB J* 19: 258–260, 2005.
67. **Takaki M, Nakahara H, Kawatani Y, Utsumi K, Suga H.** No suppression of respiratory function of mitochondria isolated from the hearts of anesthetized rats with high-dose pentobarbital sodium. *Jpn J Physiol* 47: 87–92, 1997.
68. **Toien O, Drew KL, Chao ML, Rice ME.** Ascorbate dynamics and oxygen consumption during arousal from hibernation in Arctic ground squirrels. *Am J Physiol Regul Integr Comp Physiol* 281: R572–R583, 2001.
69. **Trounce IA, Kim YL, Jun AS, Wallace DC.** Assessment of mitochondrial oxidative phosphorylation in patient muscle biopsies, lymphoblasts, and transmitochondrial cell lines. *Methods Enzymol* 264: 484–509, 1996.
70. **Van Voorhies WA.** Metabolism and lifespan. *Exp Gerontol* 36: 55–64, 2001.
71. **Wilkinson GS, South JM.** Life history, ecology and longevity in bats. *Aging Cell* 1: 124–131, 2002.
72. **Wu BJ, Hulbert AJ, Storlien LH, Else PL.** Membrane lipids and sodium pumps of cattle and crocodiles: an experimental test of the membrane pacemaker theory of metabolism. *Am J Physiol Regul Integr Comp Physiol* 287: R633–R641, 2004.